



Semarak International Journal of Applied Sciences and Engineering Technology

Journal homepage:
<https://semarakilmu.my/index.php/sijaset/index>
ISSN: 3030-5314



Influence of [EMIM][OOF] Ionic Liquid on the electrical and Structural Properties of Gel Polymer Electrolytes

Norshahirah Mohamad Saidi^{1,*}, Nurhafizah Hasim¹, Nur Hidayah Ahmad¹, Chetna Tyagi², Suresh Thanakodi³

¹ Department of Physics, Faculty of Science, Universiti Teknologi Malaysia, 81310 Skudai, Johor, Malaysia

² Department of Applied Sciences, The NorthCap University, Gurugram 122017, India

³ Department of Science and Maritime Technology, Faculty of Science and Defence Technology, Universiti Pertahanan Nasional Malaysia, 57000 Kuala Lumpur, Malaysia

ARTICLE INFO

Article history:

Received 23 September 2025

Received in revised form 23 October 2025

Accepted 28 October 2025

Available online 30 October 2025

Keywords:

Ionic liquid; Gel polymer electrolyte;
Electrochemical impedance
spectroscopy, Ionic conductivity

ABSTRACT

The growing demand for sustainable and efficient energy storage devices underscores the urgent need for safer and higher-performing electrolytes. Conventional liquid electrolytes offer high ionic conductivity but pose safety and leakage risks, while solid polymer electrolytes often suffer from limited ion mobility and poor interfacial contact. To overcome these limitations, this study investigates the effect of incorporating the ionic liquid 1-ethyl-3-methylimidazolium trifluoromethanesulfonate ([EMIM][OTf]) into a gel polymer electrolyte based on poly(1-vinylpyrrolidone-co-vinyl acetate) [P(VP-co-VAc)]. The objective of this work is to examine how varying the ionic liquid content influences the electrical and structural properties of the electrolyte. By optimizing the composition, a maximum ionic conductivity of 4.92×10^{-3} S/cm was achieved at 20 wt.% [EMIM][OTf]. X-ray diffraction analysis revealed that the improved conductivity is associated with reduced crystallinity, which facilitates ion transport. This study offers new insights into the role of [EMIM][OTf] in enhancing the amorphous character and ion mobility of P(VP-co-VAc)-based electrolytes, thereby contributing to the design of safer and more efficient gel polymer electrolytes for advanced energy storage applications.

1. Introduction

The urgent need to reduce greenhouse gas emissions and transition to sustainable energy sources has gained significant attention. The International Energy Agency (IEA) underscores the importance of shifting to low-carbon electricity sources, especially renewable energy, to lessen the environmental impact of increasing electricity demand. Consequently, investments in renewable energy technologies such as wind and solar power have surged, as these are expected to play a crucial role in meeting the growing electricity needs. Additionally, the integration of energy storage devices

* Corresponding author.

E-mail address: Norshahirah.ms@utm.my

can improve the efficiency, reliability, and sustainability of the energy system by allowing excess power generated from renewable sources to be stored [1–3].

Energy storage devices generally consist of electrodes and electrolytes, where the electrolyte serves as the ion transport medium. Conventional liquid electrolytes based on organic solvents exhibit high ionic conductivity but pose significant safety risks such as flammability, leakage, and instability at elevated temperatures [4–6][7]. To mitigate these issues, solid-state polymer electrolytes (PEs) have been explored owing to their flexibility, non-volatility, and improved safety [8–10]. Nevertheless, their low room-temperature ionic conductivity (10^{-8} – 10^{-5} S cm⁻¹) and poor interfacial contact with electrodes limit their electrochemical performance. Gel polymer electrolytes (GPEs), which combine the mechanical stability of solid PEs with the ionic mobility of liquids, offer a promising alternative, typically achieving conductivities in the range of 10^{-5} – 10^{-3} S cm⁻¹ [11,12][13].

To further enhance the ionic conductivity and electrochemical stability of GPEs, the incorporation of ionic liquids (ILs) has gained significant attention [14][15,16]. ILs are molten salts with negligible vapor pressure, high ionic content, and wide electrochemical windows, making them suitable candidates for next-generation electrolytes. Previous studies have primarily focused on ILs such as [BMIM][PF₆] and [EMIM][BF₄]; however, these systems often face limitations including phase separation, reduced mechanical integrity, or restricted ion transport at high IL loadings [17,18]. The triflate-based ionic liquid, 1-ethyl-3-methylimidazolium trifluoromethanesulfonate ([EMIM][OTf]), offers higher thermal and electrochemical stability, yet its interaction with copolymer hosts such as poly(1-vinylpyrrolidone-co-vinyl acetate) [P(VP-co-VAc)] has not been systematically investigated.

Therefore, the objective of this study is to examine the influence of [EMIM][OTf] on the electrical and structural properties of P(VP-co-VAc)-based gel polymer electrolytes, focusing on the relationship between ionic liquid content, crystallinity, and ionic conductivity. This work uniquely explores the synergistic effects of [EMIM][OTf] and the P(VP-co-VAc) copolymer system, demonstrating how an optimal IL concentration can enhance ion transport by promoting amorphous regions within the polymer matrix. The findings contribute new insights toward the rational design of high-performance, safer gel electrolytes for energy storage applications.

2. Experimental Methodology

2.1 Material

Poly (1-vinylpyrrolidone-co-vinyl acetate) P(VP-co-VAc), sodium trifluoromethanesulfonate (NaOTf), ethylene carbonate (EC), propylene carbonate (PC), and 1-ethyl-3-methylimidazolium trifluoromethanesulfonate (EMIM OTf) ionic liquid were purchased from Sigma-Aldrich, Malaysia.

2.2 Formulation of polymer electrolytes-employed EMIM OTf and Characterizations

Polymer electrolytes were formulated using a gelation technique by mixing 0.5 g of P(VP-co-VAc) into a solution containing 0.5 g of NaOTf dissolved in 1.0 g of an EC:PC binary solvent in an equal ratio. After P(VP-co-VAc) was fully dissolved in the solution under stirring and heating at 40 °C, 10 wt. % of the ionic liquid EMIM OTf was added dropwise to the mixture. The mixtures were then stirred for 1 hour at 40 °C until homogeneous gels were obtained. The polymer electrolytes were then cooled to room temperature and were ready for testing. This experiment was repeated using different wt. % of the ionic liquid EMIM OTf, as shown in Table 1.

Table 1

Composition of formulated polymer electrolytes

Electrolytes	P(VP-co-VAc), wt. %	NaOTf, wt. %	EMIM OTf, wt. %
PPV-S	50	50	-
PPVIL-10	45	45	10
PPVIL-20	40	40	20
PPVIL-30	35	35	30
PPVIL-40	30	30	40

The formulated polymer electrolytes were then prepared for testing using electrochemical impedance spectroscopy (EIS) analysis. The EIS studies were conducted to evaluate the electrical performance of the polymer electrolytes based on their conductivity values. EIS testing was carried out using a HIOKI LCR Hi-Tester Model 3532-50 over a frequency range of 50 Hz to 5 MHz at 25 °C. The samples were placed into a coin cell with a hole area, A , of 2.0 cm² and a thickness, l , of 2.9 mm. The samples were then positioned between two stainless steel blocking electrodes. The conductivity, σ , was calculated using Eq. 1.

$$\sigma = \frac{l}{R_b \times A} \quad (1)$$

where, R_b is bulk resistance (Ω) of the samples obtained from EIS studies.

The structural crystallinity and phase purity of the polymer electrolytes were confirmed by an Empyrean X-ray diffractometer (PANalytical). This analysis was done from the 2θ range of 5° to 80°. The crystallite size broadening of the samples can be calculated by using the Scherrer equation as follow:

$$B_{2\theta} = \frac{K\lambda}{\beta \cos \theta} \quad (2)$$

where $B_{2\theta}$ is the average of the ordered (crystalline) domain, K is a dimensionless shape factor (typically $K = 0.9$), λ is the X-ray wavelength, θ is the line broadening at half the maximum intensity (FWHM), and ϑ is the Bragg angle.

3. Results and Discussion

3.1 Electrochemical analysis of the polymer electrolytes

Figure 1 shows the Cole-Cole impedance plots obtained from the electrochemical impedance spectroscopy (EIS) analysis. In the graph, the intersection with the real axis represents the bulk resistance of the samples [19]. The bulk resistance (R_b) values for the polymer electrolytes without ionic liquid (PPV-S) and those with ionic liquid (PPVIL-10, PPVIL-20, PPVIL-30, and PPVIL-40) are 102.77, 32.72, 28.50, 29.77, and 39.06 Ω , respectively, as summarized in Table 2.

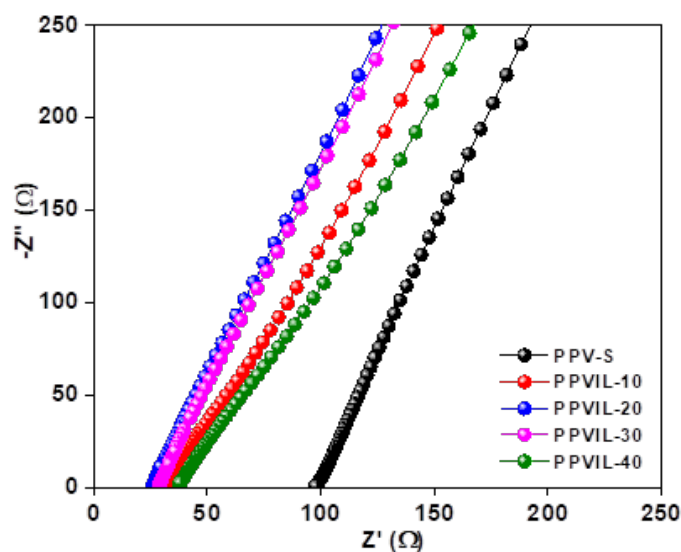


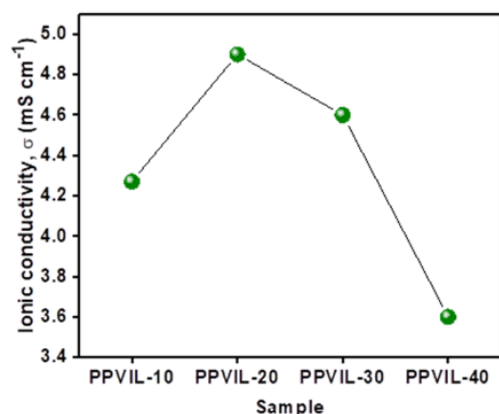
Fig. 1. Cole-Cole impedance plot of the polymer electrolytes-employed ionic liquid

Table 2

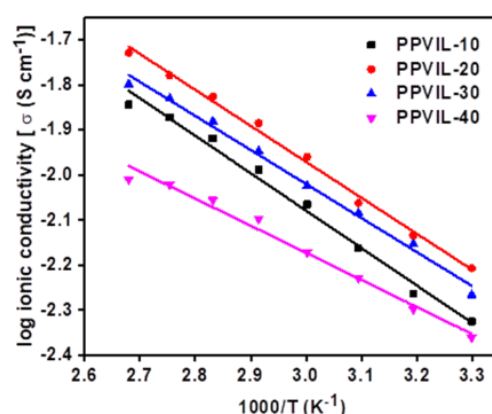
Electrochemical parameters of polymer electrolytes-employed ionic liquid

Electrolytes	Bulk resistance, R_b (Ω)	Ionic conductivity, σ (S/cm)	Activation energy, E_a (eV)	R-squared
PPV-S	102.77	1.21×10^{-3}	0.190	0.996
PPVIL-10	32.72	4.28×10^{-3}	0.186	0.988
PPVIL-20	28.50	4.92×10^{-3}	0.172	0.996
igPPVIL-30	29.77	4.70×10^{-3}	0.177	0.995
PPVIL-40	39.06	3.58×10^{-3}	0.189	0.994

The conductivity, σ , was calculated using Eq. (1). The addition of [EMIM][OTf] markedly increased ionic conductivity, reaching a maximum of $4.92 \times 10^{-3} \text{ S cm}^{-1}$ for PPVIL-20. This enhancement can be attributed not only to the reduction in polymer crystallinity but also to the specific ion–polymer interactions introduced by the ionic liquid. Mechanistically, [EMIM][OTf] functions as a dual charge carrier system, where both the cation ([EMIM]⁺) and anion ([OTf][−]) participate in ion transport. When incorporated into the polymer matrix, the bulky asymmetric [EMIM]⁺ cations interact with the carbonyl (C=O) and lactam (−C−N−) groups of P(VP-co-VAc) through ion–dipole interactions. These interactions weaken the intra- and intermolecular hydrogen bonding within the polymer chains, enhancing their segmental mobility. The [OTf][−] anions, being weakly coordinating, further increase the number of mobile charge carriers by dissociating Na⁺ ions from the NaOTf salt and forming transient ion pairs with [EMIM]⁺ [20][21][22].



(a) Ionic conductivity trend



(b) Linear relationship between log ionic conductivity and inverse temperature (1000/T)

Fig. 2. Electrochemical impedance spectroscopy (EIS) analysis of the polymer electrolytes-employed ionic liquid; (a) Ionic conductivity trend and (b) Linear relationship between log ionic conductivity and inverse temperature (1000/T).

Such coordination disrupts local order in the polymer backbone, leading to increased amorphous character and the formation of continuous ion-conduction pathways. Consequently, charge transport occurs predominantly via the polymer-segmental motion–assisted ion hopping mechanism, as supported by the Arrhenius-type temperature dependence (Figure 2b). The linear behavior with $R^2 > 0.99$ (approximately ~ 1) confirms thermally activated conduction, where increased chain mobility at higher temperatures facilitates easier migration of charge carriers [23][24]. The activation energy (E_a) for ion migration can be calculated using the Arrhenius equation as follows:

$$\sigma = \sigma_0 \exp(E_a/RT) \quad (3)$$

where σ_0 is the pre-exponential factor, R is the gas constant (J/Kmol), and T is the temperature (K). The E_a values for all the electrolyte samples are reported in Table 2.

The observed conductivity trend (PPVIL-20 > PPVIL-30 > PPVIL-10 > PPVIL-40 > PPV-S) indicates an optimal ionic-liquid concentration around 20 wt.%. Beyond this level, excess [EMIM][OTf] leads to ion-pair aggregation and micro-domain formation, which reduce the number of free mobile ions and block conduction pathways [25]. The lowest E_a value (0.172 eV) for PPVIL-20 further supports that ion motion is facilitated through a combination of segmental relaxation and local ion hopping, requiring less energy for migration compared to other compositions.

3.2 Structural properties of the formulated polymer electrolytes

The addition of the ionic liquid EMIM OTf plays a major role in reducing the degree of crystallinity of the host polymer, thus enhancing ion transport and the overall performance of the polymer electrolytes. Figure 3 displays the XRD spectra of the P(VP-co-VAc) mixture in binary solvents (labeled as PPV), the polymer electrolyte without ionic liquid (PPV-S), and the optimal polymer electrolyte containing 20 wt.% of EMIM OTf (PPVIL-20). According to the literature, pure P(VP-co-VAc) is typically semicrystalline due to its non-uniform molecular weight, showing two broad humps in its diffractogram [25]. However, only a broad peak is observed in the XRD spectrum after dissolving the polymer in the binary solvent of EC:PC, indicating an increase in the disordered

phase of the samples. The original broad peak observed in PPV has shifted in the spectra of PPV-S and PPVIL-20, as shown in Figure 3. This shift in the broad peaks of the pure polymer may be due to the disruption of the polymer's microstructure after mixing with salts and ionic liquids. Additionally, mixing the polymer with the solvent improves molecular crosslinking, leading to the formation of more homogeneous gels due to the plasticizing effect of the solvents [26]. Thus, the addition of the solvent reduces the polymer's tendency to crystallize, resulting in a more flexible polymer matrix compared to the pure polymer powder [27]. Table 3 summarizes the peak parameters (2θ and FWHM). The increase in FWHM from 4.01° (PPV) to 4.76° (PPVIL-20) corresponds to reduced degree of crystallinity and increased amorphous phase.

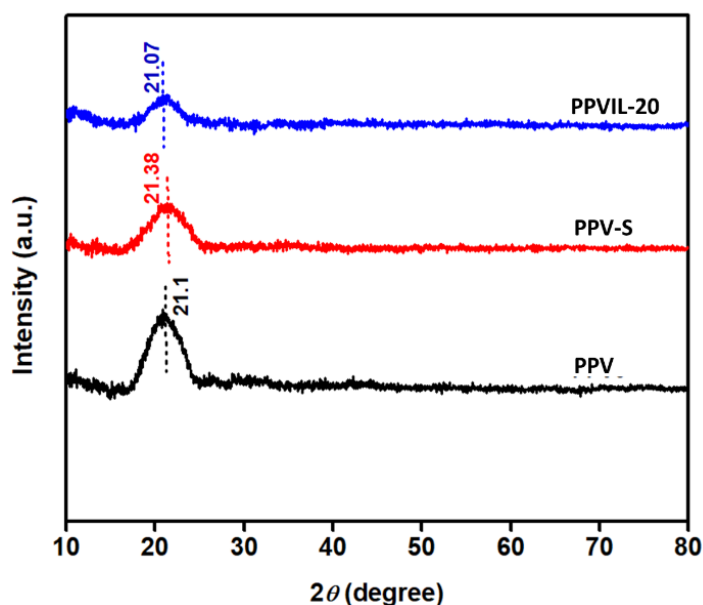


Fig. 3. Comparison of XRD spectra between PPV, PPV-S and PPVIL-20

Table 3

Parameters of FWHM, 2θ and T obtained from XRD spectrum

Electrolytes	FWHM ($^\circ$)	2θ ($^\circ$)
PPV	4.01	10.55
PPV-S	4.53	10.70
PPVIL-20	4.76	10.54

The structural modification is consistent with the conductivity enhancement observed in EIS. The ionic liquid interacts with both the PVP and PVAc segments: the imidazolium cation of [EMIM][OTf] forms transient complexes with carbonyl oxygen atoms, while the [OTf]⁻ anion disrupts the polymer-salt electrostatic network, creating a more open polymer configuration. This molecular-level disorder increases the number of hopping sites and facilitates long-range ion diffusion. Moreover, the bulky [EMIM]⁺ cation acts as a molecular spacer, preventing polymer chain re-packing and stabilizing the amorphous phase even at higher IL concentrations. These

cooperative structural and dynamic effects explain why the optimum 20 wt.% [EMIM][OTf] sample shows both the lowest activation energy and highest ionic conductivity.

4. Conclusions

This study demonstrates that incorporating the ionic liquid 1-ethyl-3-methylimidazolium trifluoromethanesulfonate ([EMIM][OTf]) into a P(VP-co-VAc)-based gel polymer electrolyte substantially enhances ionic conductivity and modifies the polymer microstructure. The optimum composition containing 20 wt.% [EMIM][OTf] exhibited the highest conductivity of $4.92 \times 10^{-3} \text{ S cm}^{-1}$ and the lowest activation energy of 0.172 eV. These improvements originate from the dual function of [EMIM][OTf]: (i) its ability to plasticize the polymer matrix and increase chain segmental mobility, and (ii) its capability to dissociate Na^+ ions from NaOTf salt through ion–dipole interactions between $[\text{EMIM}]^+ / [\text{OTf}]^-$ and the carbonyl or lactam groups of the copolymer. The combined effects enhance amorphousness, facilitate ion hopping, and create more continuous transport pathways within the polymer matrix. Beyond the quantitative improvements, these results provide theoretical insight into the ion-transport mechanism of imidazolium-based ionic liquids in copolymer systems; highlighting the interplay between molecular interactions, polymer dynamics, and charge mobility. The observed optimum at 20 wt.% suggests a critical balance between ion dissociation and aggregation, where excessive [EMIM][OTf] leads to ionic clustering and reduced conductivity. For future work, the concentration of the ionic liquid and the polymer composition should be further optimized to improve both conductivity and mechanical strength. Additional studies should evaluate the electrolyte's mechanical durability, cycling performance, and long-term stability.

Acknowledgement

This research was funded by the UTM Encouragement Research (PY/2024/01390).

References

- [1] M.-C. Lin, M. Gong, B. Lu, Y. Wu, D.-Y. Wang, M. Guan, M. Angell, C. Chen, J. Yang, B.-J. Hwang, H. Dai, An ultrafast rechargeable aluminium-ion battery, *Nature*. 520 (2015) 324–328. <https://doi.org/10.1038/nature14340>.
- [2] Z. Lin, M. Mao, C. Yang, Y. Tong, Q. Li, J. Yue, G. Yang, Q. Zhang, L. Hong, X. Yu, L. Gu, Y.-S. Hu, H. Li, X. Huang, L. Suo, L. Chen, Amorphous anion-rich titanium polysulfides for aluminum-ion batteries, *Sci. Adv.* 7 (2024) eabg6314. <https://doi.org/10.1126/sciadv.abg6314>.
- [3] H. Zhang, X. Liu, H. Li, I. Hasa, S. Passerini, Challenges and Strategies for High-Energy Aqueous Electrolyte Rechargeable Batteries, *Angew. Chemie Int. Ed.* 60 (2021) 598–616. <https://doi.org/https://doi.org/10.1002/anie.202004433>.
- [4] K. Vignarooban, R. Kushagra, A. Elango, P. Badami, B.-E. Mellander, X. Xu, T.G. Tucker, C. Nam, A.M. Kannan, Current trends and future challenges of electrolytes for sodium-ion batteries, *Int. J. Hydrogen Energy*. 41 (2016) 2829–2846. <https://doi.org/https://doi.org/10.1016/j.ijhydene.2015.12.090>.
- [5] L. Chen, L. Cao, X. Ji, S. Hou, Q. Li, J. Chen, C. Yang, N. Eidson, C. Wang, Enabling safe aqueous lithium ion open batteries by suppressing oxygen reduction reaction, *Nat. Commun.* 11 (2020) 2638. <https://doi.org/10.1038/s41467-020-16460-w>.
- [6] X. Wang, B. Zhang, J. Feng, L. Wang, B. Wu, J. Zhang, X. Ou, F. Hou, J. Liang, Cu-MOF-derived and porous $\text{Cu}_0.26\text{V}_2\text{O}_5/\text{C}$ composite cathode for aqueous zinc-ion batteries, *Sustain. Mater. Technol.* 26 (2020) e00236. <https://doi.org/https://doi.org/10.1016/j.susmat.2020.e00236>.
- [7] Y. Liu, Q. Liu, L. Xin, Y. Liu, F. Yang, E.A. Stach, J. Xie, Making Li-metal electrodes rechargeable by controlling the dendrite growth direction, *Nat. Energy*. 2 (2017) 17083. <https://doi.org/10.1038/nenergy.2017.83>.
- [8] R. Gonçalves, D. Miranda, A.M. Almeida, M.M. Silva, J.M. Meseguer-Dueñas, J.L.G. Ribelles, S. Lanceros-Méndez, C.M. Costa, Solid polymer electrolytes based on lithium bis(trifluoromethanesulfonyl)imide/poly(vinylidene fluoride-co-hexafluoropropylene) for safer rechargeable lithium-ion batteries, *Sustain. Mater. Technol.* 21 (2019) e00104. <https://doi.org/https://doi.org/10.1016/j.susmat.2019.e00104>.
- [9] W. Zhang, J. Nie, F. Li, Z.L. Wang, C. Sun, A durable and safe solid-state lithium battery with a hybrid electrolyte

- membrane, *Nano Energy*. 45 (2018) 413–419. <https://doi.org/https://doi.org/10.1016/j.nanoen.2018.01.028>.
- [10] X. Ban, W. Zhang, N. Chen, C. Sun, A High-Performance and Durable Poly(ethylene oxide)-Based Composite Solid Electrolyte for All Solid-State Lithium Battery, *J. Phys. Chem. C*. 122 (2018) 9852–9858. <https://doi.org/10.1021/acs.jpcc.8b02556>.
- [11] H. Yang, N. Wu, Ionic conductivity and ion transport mechanisms of solid-state lithium-ion battery electrolytes: A review, *Energy Sci. Eng.* 10 (2022) 1643–1671. <https://doi.org/https://doi.org/10.1002/ese3.1163>.
- [12] J.G. Kim, B. Son, S. Mukherjee, N. Schuppert, A. Bates, O. Kwon, M.J. Choi, H.Y. Chung, S. Park, A review of lithium and non-lithium based solid state batteries, *J. Power Sources*. 282 (2015) 299–322. <https://doi.org/https://doi.org/10.1016/j.jpowsour.2015.02.054>.
- [13] J. Castillo, A. Santiago, X. Judez, I. Garbayo, J.A. Coca Clemente, M.C. Morant-Miñana, A. Villaverde, J.A. González-Marcos, H. Zhang, M. Armand, C. Li, Safe, Flexible, and High-Performing Gel-Polymer Electrolyte for Rechargeable Lithium Metal Batteries, *Chem. Mater.* 33 (2021) 8812–8821. <https://doi.org/10.1021/acs.chemmater.1c02952>.
- [14] W. Zhou, M. Zhang, X. Kong, W. Huang, Q. Zhang, Recent Advance in Ionic-Liquid-Based Electrolytes for Rechargeable Metal-Ion Batteries, *Adv. Sci.* 8 (2021) 2004490. <https://doi.org/https://doi.org/10.1002/advs.202004490>.
- [15] Y.-C. Tseng, S.-H. Hsiang, C.-H. Tsao, H. Teng, S.-S. Hou, J.-S. Jan, In situ formation of polymer electrolytes using a dicationic imidazolium cross-linker for high-performance lithium ion batteries, *J. Mater. Chem. A*. 9 (2021) 5796–5806. <https://doi.org/10.1039/D0TA09249E>.
- [16] N. Zhu, K. Zhang, F. Wu, Y. Bai, C. Wu, Ionic Liquid-Based Electrolytes for Aluminum/Magnesium/Sodium-Ion Batteries, *Energy Mater. Adv.* 2021 (2024). <https://doi.org/10.34133/2021/9204217>.
- [17] M.Z. Dzulkiply, J. Karim, A. Ahmad, N.A. Dzulkurnain, M.S. Su'ait, M. Yoshizawa-Fujita, L.T. Khoon, N.H. Hassan, The influences of 1-butyl-3-methylimidazolium tetrafluoroborate on electrochemical, thermal and structural studies as ionic liquid gel polymer electrolyte, *Polymers (Basel)*. 13 (2021). <https://doi.org/10.3390/polym13081277>.
- [18] J. Tang, R. Muchakayala, S. Song, M. Wang, K.N. Kumar, Effect of EMIMBF₄ ionic liquid addition on the structure and ionic conductivity of LiBF₄-complexed PVdF-HFP polymer electrolyte films, *Polym. Test.* 50 (2016) 247–254. <https://doi.org/10.1016/j.polymertesting.2016.01.023>.
- [19] S.I.A. Halim, C.H. Chan, J. Apotheker, Basics of teaching electrochemical impedance spectroscopy of electrolytes for ion-rechargeable batteries – part 2: dielectric response of (non-) polymer electrolytes, *Chem. Teach. Int.* 3 (2021) 117–129. <https://doi.org/10.1515/cti-2020-0018>.
- [20] A. Syairah, M.H. Khanmirzaei, N.M. Saidi, N.K. Farhana, S. Ramesh, K. Ramesh, S. Ramesh, Effect of different imidazolium-based ionic liquids on gel polymer electrolytes for dye-sensitized solar cells, *Ionics (Kiel)*. (2018). <https://doi.org/10.1007/s11581-018-2603-6>.
- [21] C.Y. Tan, N.K. Farhana, N.M. Saidi, S. Ramesh, K. Ramesh, Conductivity, dielectric studies and structural properties of P(VA-co-PE) and its application in dye sensitized solar cell, *Org. Electron.* 56 (2018) 116–124. <https://doi.org/10.1016/j.orgel.2018.02.007>.
- [22] N.M. Saidi, H.M. Ng, F.S. Omar, S. Bashir, K. Ramesh, S. Ramesh, Polyacrylonitrile–poly(1-vinyl pyrrolidone-co-vinyl acetate) blend based gel polymer electrolytes incorporated with sodium iodide salt for dye-sensitized solar cell applications, *J. Appl. Polym. Sci.* 136 (2019) 47810. <https://doi.org/10.1002/app.47810>.
- [23] N. Zebardastan, M.H. Khanmirzaei, S. Ramesh, K. Ramesh, Performance enhancement of poly(vinylidene fluoride-co-hexafluoro propylene)/polyethylene oxide based nanocomposite polymer electrolyte with ZnO nanofiller for dye-sensitized solar cell, *Org. Electron.* 49 (2017) 292–299. <https://doi.org/10.1016/j.orgel.2017.06.062>.
- [24] Z.L. Goh, N.M. Saidi, N.K. Farhana, S. Bashir, J. Iqbal, K. Ramesh, S. Ramesh, S. Wageh, A. Kalam, Sonochemically synthesized cobalt oxide nanoparticles as an additive for natural polymer iodide electrolyte based dye-sensitized solar cells, *Sustain. Energy Technol. Assessments*. 49 (2022) 101746. <https://doi.org/10.1016/j.seta.2021.101746>.
- [25] S.N.F. Yusuf, A.D. Azzahari, V. Selvanathan, R. Yahya, M.A. Careem, A.K. Arof, Improvement of N-phthaloylchitosan based gel polymer electrolyte in dye-sensitized solar cells using a binary salt system, *Carbohydr. Polym.* 157 (2017) 938–944. <https://doi.org/10.1016/j.carbpol.2016.10.032>.
- [26] T. Ouchi, M. Yamazaki, T. Maeda, A. Hotta, Mechanical property of polypropylene gels associated with that of molten polypropylenes, *Gels*. 7 (2021) 99. <https://doi.org/10.3390/gels7030099>.
- [27] J. Li, A.B. Huckleby, M. Zhang, The enhanced power factor of multi-walled carbon nanotube/stabilized polyacrylonitrile composites due to the partially conjugated structure, *J. Mater.* 7 (2021) 51–58. <https://doi.org/10.1016/j.jmat.2020.08.002>.